Mausam. (1996), 47, 4, 355-368

551.46.062.8 : 551.553.21 (267.37)

Observed variability in the current field during summer monsoon experiments : Arabian Sea

R. R. RAO, K. V. SANIL KUMAR and BASIL MATHEW
Naval Physical & Oceanographic Laboratory, Cochin
(Received 18 April 1994. Modified 29 March 1996)

सार — मानसून-77 तथा मोनेक्स-79 के क्षेत्रीय प्रयोगों के दौरान पूर्व यू०एस०एस०आर० के स्थाई पोत का बहुभुज आकृतियों से प्राप्त हुए 'मूर्ड' धारामीटर रिकार्ड द्वारा सुलभ हुए अल्प (1-2 सप्ताह) समय अनुक्रम के उपयोग द्वारा अरब सागर के चुने हुए स्थानों पर धारा क्षेत्र की ऊपरी तह में प्रेक्षित अल्पावधि अस्थिरता की जांच की गई है। 200 मी. ऊपर के जल कॉलम में धारा क्षेत्र के प्रेक्षित स्वरूप और उसकी अस्थिरता का वर्णन करने के लिए सतही पवन उप-सतही तापमान और लवणता से संबंधित अनुपूरक समय श्रृंखला के आंकड़ा सेट का भी उपयोग किया गया है। मानसून-77 के दौरान ग्रीष्म मानसून के आरम्भ और उसके आगे बढ़ने के साथ मध्य अरब सागर में ऊष्मीय प्रवृत्ति मिश्रित सतही तह का सघनन तथा शीतलन दर्शाती है जबकि मोनेक्स-79 के आरम्भ से पूर्व की अवधि में पश्चिमी और दक्षिणी मध्य अरब सागर में सह-संबंधी विभिन्नता आंशिक थी। केवल मानसून-77 की प्रगति की अवधि में एकमैन संतुलन मिश्रित तह में सीमित प्रतीत हुआ है तथा मोनेक्स-79 के आरम्भ तथा पूर्व आरम्भ की अवधि में यह विद्यमान नहीं था जो धारा क्षेत्र को प्रभावित करने वाली आंतरिक महासागरीय गतिकी की महत्ता दर्शाता है। धारा संबंधी अधिकांश रिकार्ड समूचे 200 मी. जल कॉलम तक फैली हुई अधिस्थापित दोलनों वाली सुदृढ़ संरचना का आभास कराते हैं। मानसून-77 की प्रगति की अवधि में तथा मोनेक्स-79 के आरम्भ से पूर्व की अवधि के दौरान भूमध्यरेखीय केन्द्र में भंवर विस्कासिता में असमानताओं के कारण मिश्रित स्तर से ताप-प्रवणता तक धारा के विस्तार में असामान्य कमी हुई है। मोनेक्स-79 के दौरान मानसून के आरम्भ से पहले भी भूमध्यरेखा (49° पू.) में दक्षिणी प्रवाह (100 सें.मी./सेकिंड) में प्रबल उपसतह कोर देखा गया है। घूर्णी स्पैक्ट्रल विश्लेषण से संबंधित धारा मीटर रिकार्ड की वैक्टर समय श्रृंखला, मोनेक्स-79 की तुलना में मानसून-77 के दौरान प्रवाह क्षेत्र में निष्क्रिय (इनर्शियल) दोलन अधिक स्पष्ट थे।

ABSTRACT. The observed short term variability in the current field of the upper layers at selected locations in the Arabian Sea is examined utilising the available short (1-2 weeks) time series of moored currentmeter records obtained from former USSR stationary ship polygons during MONSOON-77 and MONEX-79 field experiments. Supplementary time series data sets on surface wind, sub-surface temperature and salinity were also made use of to explain the observed structure and variability of current field in the upper 200 m water column. The thermal regime in the central Arabian Sea showed cooling and deepening of the surface mixed layer with the onset and progress of the summer monsoon during MONSOON-77 while the corresponding variability was marginal in the western and south-central Arabian Sea during pre-onset regime of MONEX-79. The Ekman balance appeared to be limited to the mixed layer, only during progress regime of MONSOON-77 and was absent during pre-onset and onset regimes of MONEX-79 suggesting the importance of internal ocean dynamics influencing the current field. Most of the current records showed rich structure with superposed oscillations extending over the entire 200 m water column. During progress regime of MONSOON-77 and at the equatorial station during pre-onset regime of MONEX-79, dramatic reduction in the current strength is noticed from mixed layer to thermocline due to differences in the eddy viscosity. During MONEX-79, a strong subsurface core of southerly flow (~100 cm/s) was noticed at the equator (49°E) even before the onset of monsoon. The vector time series of current-meter records subjected to rotary spectral analysis showed inertial oscillations in the flow regime more prominently during MONSOON-77 as compared to MONEX-79.

Key words — Summer monsoon, Currents, MONSOON-77, MONEX-79, Thermocline, Polygon area, Ekman balance.

1. Introduction

The seasonal reversing monsoons profoundly influence the annual cycle of near-surface circulation of the northern Indian Ocean. Most of the description on the spatio-temporal variability of this near-surface flow field for this area was derived from (*i*) historic ship drifts (KNMI 1952, US Navy 1976, Cutler and Swallow 1984, Rao *et al.* 1989), (*ii*) dynamic topography (Varadachari *et al.* 1968, Duing 1970, Wyrtki 1971, Rao and Sastry 1981), (*iii*) physical properties (Gopalakrishna and Sastry 1986), (*iv*) satellite imageries (Krishna Rao 1974, Legeckis 1987), (*v*) drift buoy trajectories monitored by

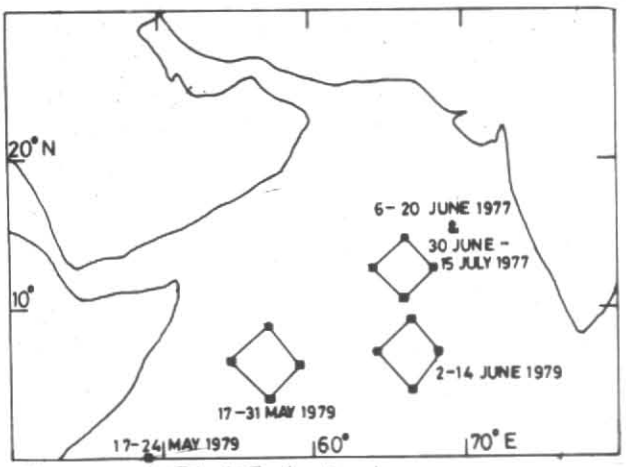

Fig. 1. Station location map

satellites (Molinari *et al.* 1990), (*vi*) direct measurements at a few selected locations (Knox 1976, Leetma and Stommel 1980, Leetma *et al.* 1982, Swallow *et al.* 1983, Gopalakrishna *et al.* 1989, Joseph *et al.* 1990, Rao *et al.* 1991, Schott *et al.* 1994 and (*vii*) models (Lighthill 1969, Cox 1970, Luther and O'Brien 1985, Anderson 1992, McCreary *et al.* 1993). However, prior to the conduct of summer monsoon experiments, practically no studies were reported based on direct current measurements in the central and eastern Arabian Sea and Bay of Bengal.

One of the major scientific objectives of the summer monsoon experiments was to understand the nature of forcing of the summer monsoon and its impact on the upper layers of the Arabian Sea and the Bay of Bengal. Accordingly field experiments were designed for the first time for time series measurements with current meter moorings from the anchored buoys in the central Arabian Sea (MONSOON-77), the equatorial (MONEX-79), the north equatorial Arabian Sea (MONEX-79) and the northern Bay of Bengal (MONSOON-77 and MONEX-79). Using some of these data sets, Ramam *et al.* (1982) and Gopalakrishna *et al.* (1989) described the observed variability of the surface winds and subsurface currents. Rao *et al.* (1991) in their first part of this study, made a detailed analysis of the observed current field in the northern Bay of Bengal during summer monsoon field experiments. In this paper, which is an extension of the authors' earlier study (1991), the observed features of near-surface flow field at all the four polygons in the Arabian Sea and at a western equatorial station are presented.

2. Data and methodology

Four ship stationary polygons, designated as M1-77 (7-19 June 1977), M2-77 (30 June-15 July 1977), M1-79 (17-31 May 1979) and M2-79 (2-14 June 1979) were deployed in the Arabian Sea (Fig. 1) by former USSR during MONSOON-77 and MONEX-79 field experiments. In addition, a solitary ship was also deployed on the equator at 49°E during M1-79. In the following discussion, the stations at northern, eastern, southern and western corners of the polygon and the equatorial station are designated as N, E, S, W and EQ respectively. Currentmeter data collected at 25, 50, 100, 150 and 200 m depths at half hourly intervals for durations of the order of 1-2 weeks are utilized in this study. These data were reported at a resolution of 1° in direction and 1 cm/s in speed (accuracy in direction ±10° and in speed ±2 cm/s). The corresponding surface wind data at 10 m height were collected at 1 or 3 hourly intervals. Data collected with bathythermograph and Nansen bottles at 3 or 6 hourly intervals are utilised to construct mean vertical profiles of temperature, salinity, density (σt) and Brunt Vaisala Frequency (N) for all the locations.

The observed current records usually exhibit oscillations of different periods. The rotary spectral analysis technique is proved to be more appropriate in determining spectral energy estimates of time series of vector current measurements compared to the Fourier analysis of zonal and meridional components to identify the sense of rotation (Gonella 1972). The currentmeter records were low pass filtered (Bloomfield 1976) with a cut off frequency at 0.093 cph (10.66 hr) to remove higher frequencies and the filtered data were subjected to rotary spectral analysis.

3. Results and discussion

The overall behaviour of the monsoon during 1977 and 1979 was contrasting. During 1977 the monsoon behaviour was above normal (Anonymous 1978) while it was below normal in 1979 (Awade *et al.* 1986). Accordingly the summer monsoonal forcing over the Arabian Sea is expected to be different for both the years. During 1977, the ships occupied the same positions in the central Arabian Sea during the onset (M1-77) and the progress regime (M2-77) of the summer monsoon which provided an unique opportunity to investigate the response of the upper ocean to variable monsoonal forcing during both the onset and progress regimes. However during 1979, the ships occupied positions in the southwestern Arabian Sea corresponding to the pre-onset regime and in the south central Arabian Sea coinciding with the onset of the monsoon.

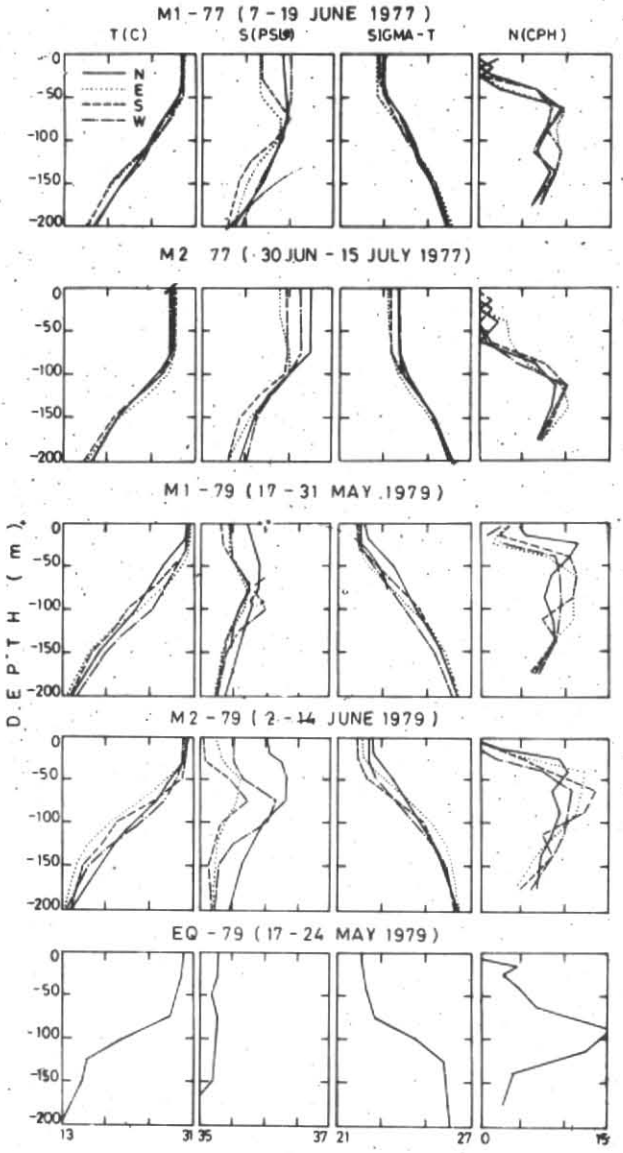

Fig. 2. Mean profiles of observed temperature, salinity and estimated σt and Brunt Vaisala Frequency (N) for MONSOON-77 and MONEX-79

3.1. *Observed mean hydrography*

The mean distributions of the vertical profiles of observed temperature, salinity and estimated σt (density) and N for all the four polygons M1-77, M2-77, M1-79 and M2-79 and at a solitary station EQ-79 during M1-79 are shown in Fig. 2. The mean temperature profiles showed deepening and cooling of the mixed layer from M1-77 to M2-77 with negligible spatial variability across the polygon (Rao 1987). During M1-79 and M2-79 the near-surface isothermal layer at all locations was warmer (~30°C) and shallower (~25-30 m) typical of pre-monsoon conditions. However, during M1-77 the vertical salinity profiles for all the stations showed some interesting spatial differences. A well defined sub-surface salinity maxima was noticed only at E and S which disappeared during M2-77 under the influence of sustained mixing caused by monsoonal winds (Rao and Sanilkumar 1991). On the other hand, all the 4 stations during M2-79 showed (and to a lesser extent during M1-79) a well defined subsurface salinity maxima corresponding to pre-monsoon conditions (Wyrtki, 1971). In general, the mixed layer at all the stations deepened by about 25 m from M1-79 to M2-79. The EQ showed altogether a different type of vertical thermo-haline structure during M1-79 not typical of the Arabian Sea. The temperature profile is characterised by layers of (*i*) near isothermal layer in the upper 75 m, (*ii*) strong thermocline between 75 and 125 m depths and (*iii*) weak thermocline below 125 m depth. This type of two layer structure is attributed to upwelling and complex current structure (Luyten and Swallow 1976) in the equatorial region. At all the stations, the shape of the σt profiles mainly resembled temperature profiles rather than the salinity profiles, suggesting that the influence of salinity on σt variability was marginal as expected for open ocean.

The Brunt Vaisala Frequency (N) is a measure of stratification of the water column. The mean profiles of N during M1-77 (Fig. 2) showed a double core maxima suggesting the presence of two different stratified layers in the thermocline which merged with the progress of the summer monsoon during M2-77 (Rao 1987). Stronger stratification was noticed in the upper thermocline during both M1-79 and M2-79 (Fig. 2).

3.2. *Short-term variability in the current field*

Direct current measurements made at half hourly intervals were utilised to describe the short term variability in the flow regime at selected depths of the topmost 200 m water column. The current-meter data were filtered to remove the variance with periods less than semi-diurnal (M2) tide, *i.e.* 12.5 hrs (0.08 cph) for plotting as sticks for all the locations [Figs. 3, 4, 5 (a) and (b) and 6 for M1-77, M2-77, M1-79 and M2-79 respectively]. The observed surface wind data were also subjected to similar processing and the wind sticks are shown in the topmost panels of these figures.

During M1-77 (Fig. 3) the surface winds were predominantly southwesterly and steady with speeds generally exceeding 10 m/s. The winds were stronger at N and W compared to those at E and S.

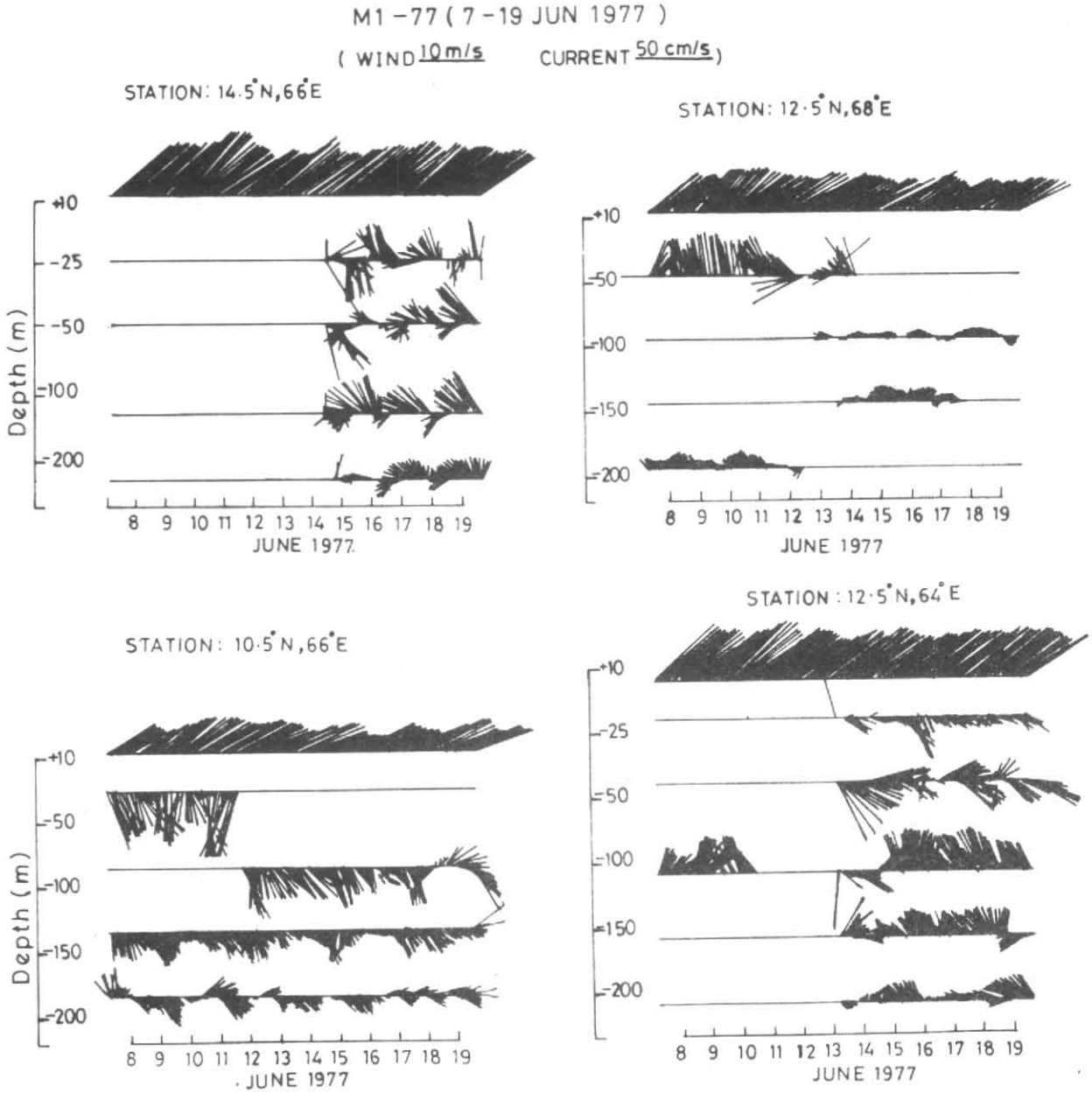

Fig. 3. Surface wind and subsurface current vectors at all four locations during M1-77

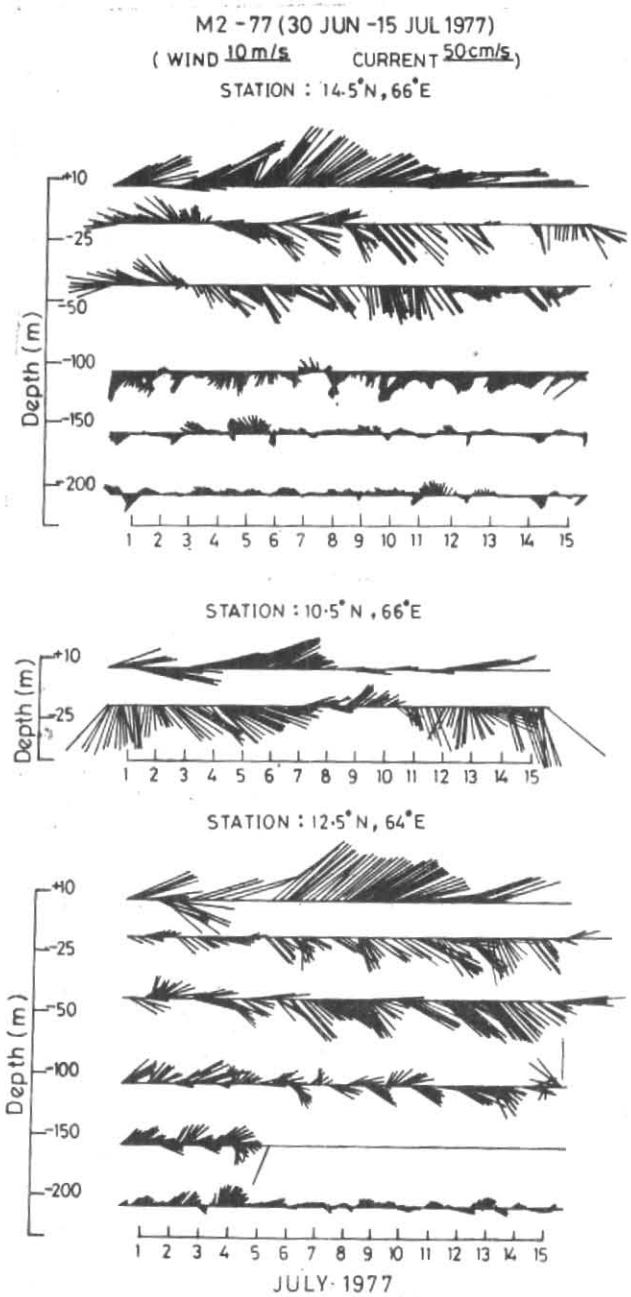

Fig. 4. Surface wind and subsurface current vectors at all four locations during M2-77

Unfortunately the current meter data at N were available only for 6 days which showed well defined oscillations about inertial period (~55 h) with good vertical coherence at all depths. The current meters at E and W also worked only for few days. The currents at E (Fig. 3) were northerly at 50 m with large reduction in speed with depth. Unlike those at N the currents at S (Fig. 3) were mostly south-southeasterly throughout with reduced strength and increased oscillatory nature with depth. At W the flow was southeasterly at 25 and 50 m and reversed to northwesterly at deeper depths. No Ekman type of flow is noticed at N, E and W stations close to the track of the onset vortex (Rao 1987) while S showed some indications of Ekman balance.

During M2-77 (Fig. 4), the wind field continued to be southwesterly and showed a pulsatory nature of the monsoon flow. In general, at all the stations, the currents were stronger within the upper 100 m (mixed layer, Fig. 2; M2-77) with a speed around 40 cm/s and were southeasterly. In contrast to M1-77, the currents in the mixed layer (upper 100 m) showed an apparent Ekman balance. However, the current speed decreased significantly below 100 m (within the thermocline) due to differences in vertical eddy viscosity in the thermocline. The flow was also more oscillatory below 100 m.

During M1-79 (Fig. 5 a), the current measurements correspond to pre-onset regime coinciding with the formation of the Somali Current System (Swallow *et al.* 1983). The oscillatory southerly surface winds were generally weak (~5 m/s) during the entire observational period at all locations typical of pre-onset conditions. The only exception was EQ-79 (Fig. 5 b) where relatively stronger winds were noticed. However currents in the upper 50 m water column were against the wind field at all stations except at N where the flow and wind directions were almost parallel. In general the currents were stronger (> 40 cm/s) both at 25 and 50 m at all locations. The current patterns also showed energetic oscillations with periods of 1-3 days at all depths. The currents at 25 and 50 m at EQ (Fig. 5 b) were against the steady surface wind field and registered a dramatic increase in strength from 40 to 120 cm/s within a week. The strongest currents were observed at 50 m depth within the near isothermal layer (Joseph *et al.* 1990). A similar strengthening is also noticed at 100 m (in the sharp thermocline) during this period. This observed strengthening can not be explained due to local wind forcing but has to be attributed to the developing eddy field in the Somali Basin. Below 100 m depth a great deal of variability is noticed in direction as reported earlier (Luyten and Swallow 1976).

The observations during M2-79 (Fig. 6) represent the transient period from pre-onset to the onset regime of the summer monsoon. The surface wind field at all the four locations is characterised by pulsatory nature and strengthened to over 10 m/s after the initial few days, when the monsoonal onset took place. At N and E, the currents at 25 m were

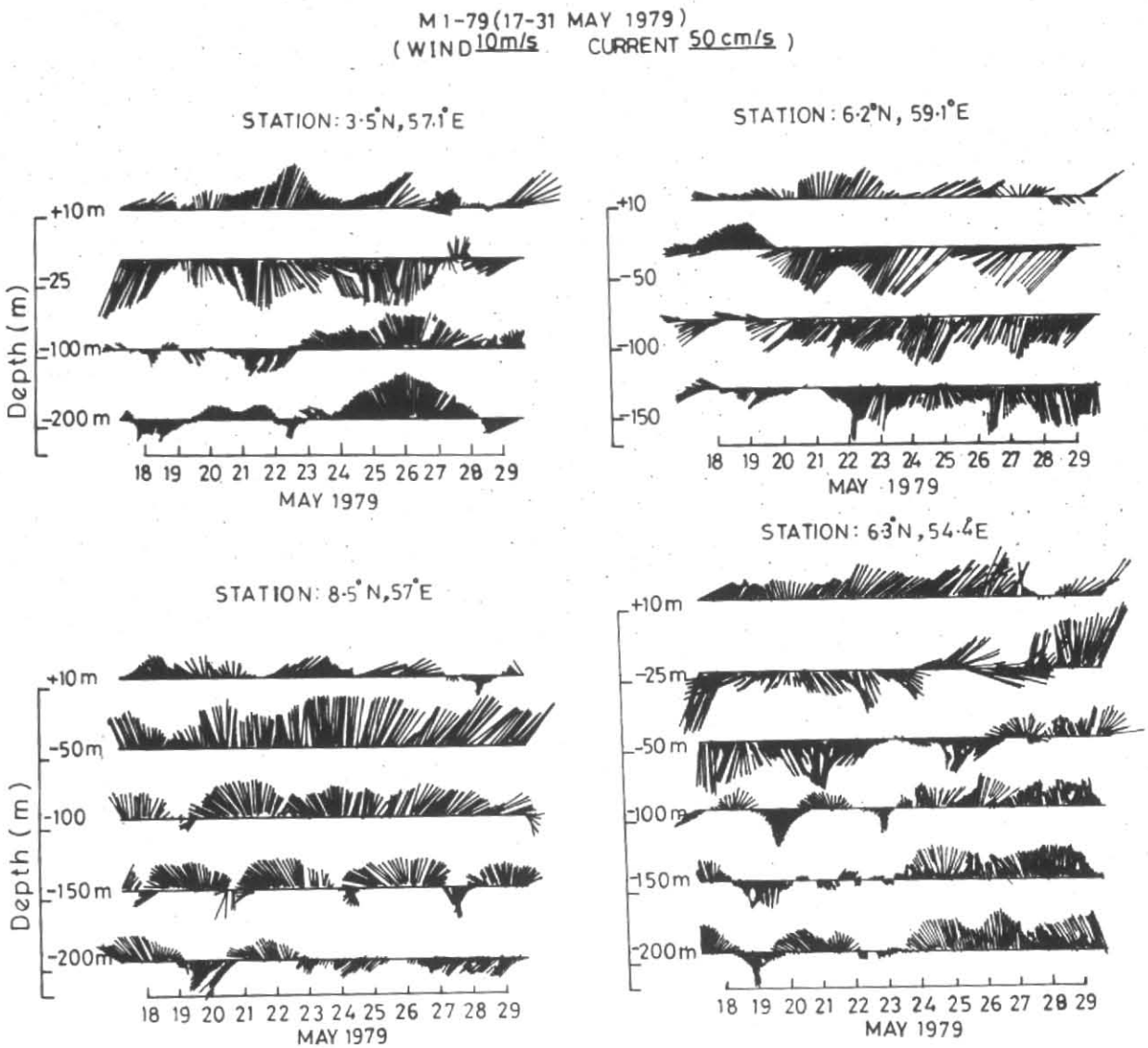

Fig. 5 (a). Surface wind and subsurface current vectors at all four locations during M1-79

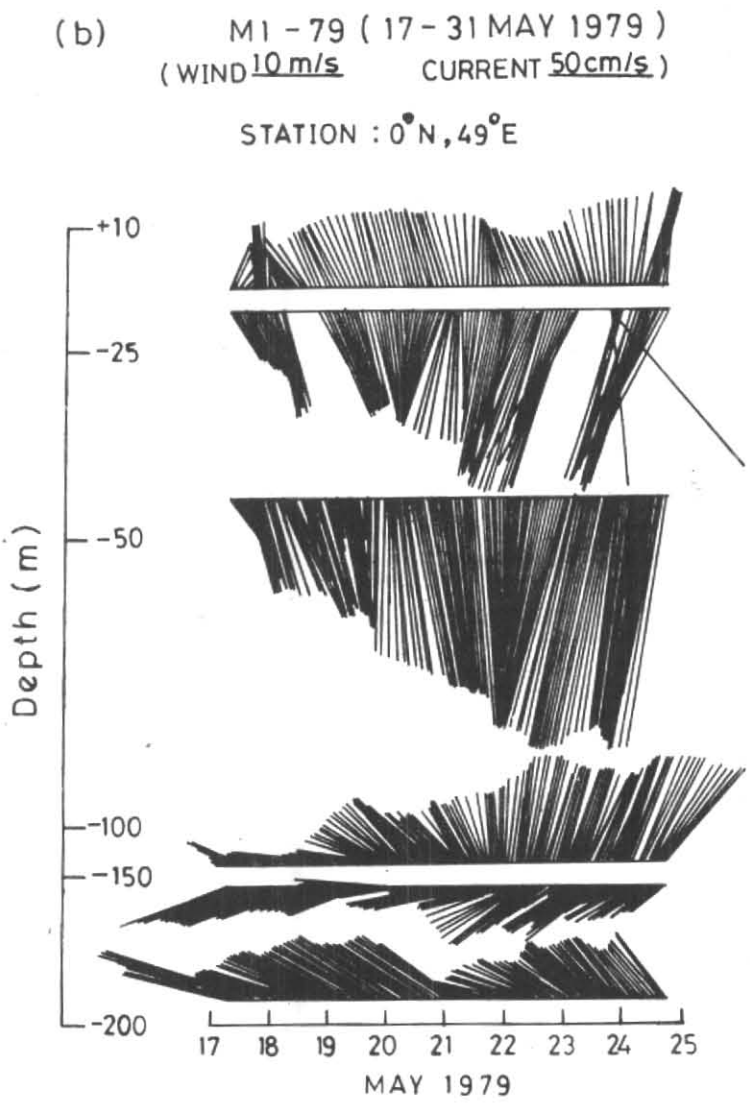

Fig. 5 (b). Surface wind and subsurface current vectors at equatorial station during M1-79

against the surface winds. The currents at N were southwesterly down to 200 m with marginal decrease in speed suggesting the absence of Ekman balance. The currents at S at 25 and 50 m were mostly southeasterly with superposed oscillatory nature. Below 50 m, the currents showed a reversal in direction at all the depths. The currents at 150 and 200 m were towards northeast embedded with synoptic scale oscillations. At 100 m depth, the currents showed a great deal of fluctuations both in direction and speed approximately representing as a transition of two opposing flows. The currents at W at 50 m were oscillatory throughout with a significant reduction in strength at 150 and 200 m depths.

3.3. *Mean wind and current patterns*

The surface wind and sub-surface current data were vectorially averaged for each observational record and the mean vectors are presented for MONSOON-77 and MONEX-79 (Fig. 7). This figure serves to provide a mean picture of the observations described above. During M1-77, M2-77 and M1-79 the surface winds were predominantly southwesterly with average speeds of 12, 10 and 5 m/s respectively. But during M2-79, the winds were westerly with a mean speed of 8 m/s. It is to be noted that within each polygon area (*i.e.* ~440 × 440 km) the surface wind field is more or less uniform both in speed and direction but the currents at each station and at each depth were mostly different from each other within the polygon area itself. Thus, the spatially coherent scales for currents were much smaller than those of surface winds. Ekman balance seems to have prevailed only at S during M1-77 and at all locations during M2-77. These features clearly demonstrate the dominance of remote and local

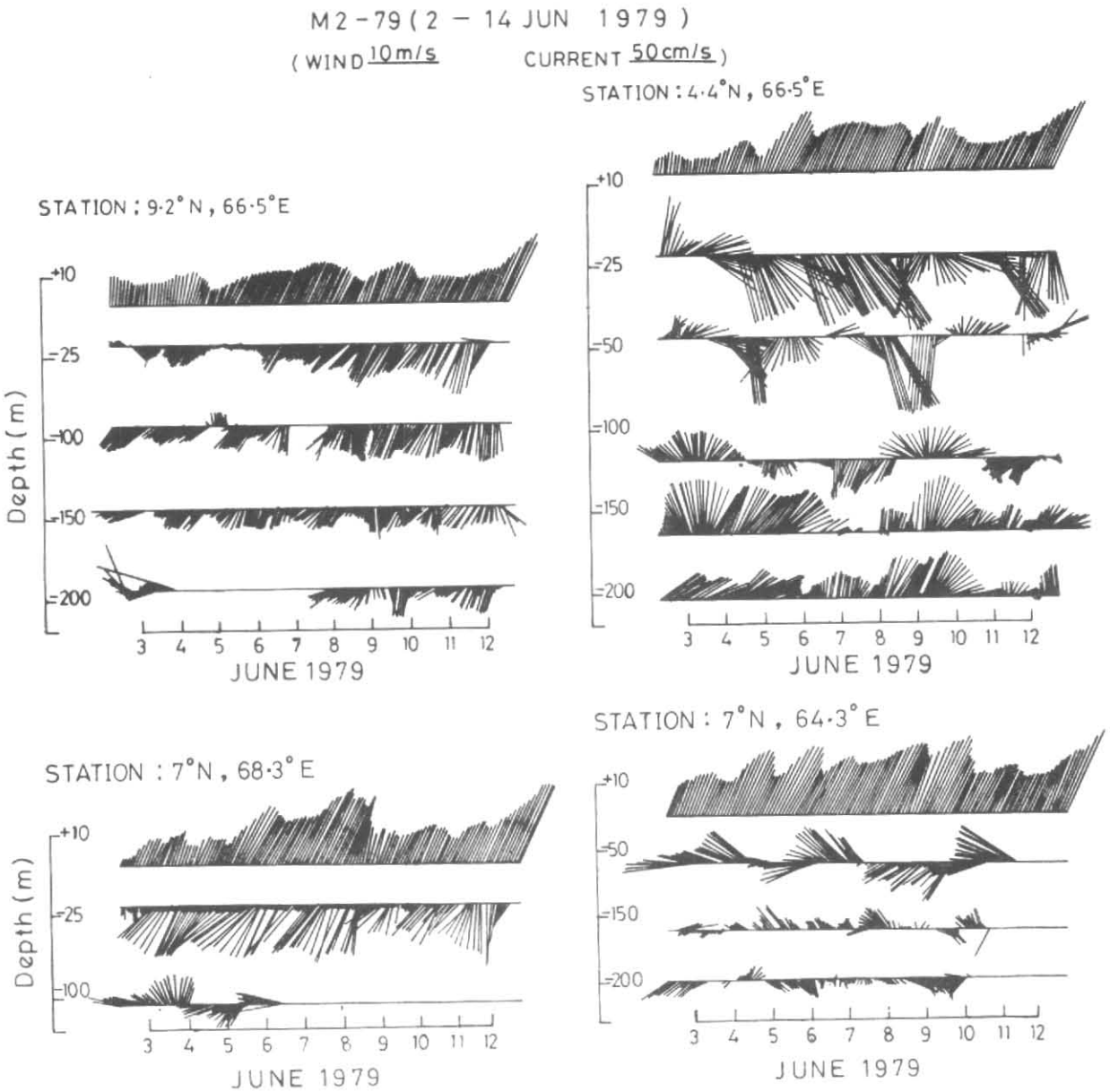

Fig. 6. Surface wind and subsurface current vectors at all four locations during M2-79

TABLE 1 (a)

	N				E				S				W			
	σu	$\overline{u}$	σv	$\overline{v}$	σu	$\overline{u}$	σv	$\overline{v}$	σu	$\overline{u}$	σv	$\overline{v}$	σu	$\overline{u}$	σv	$\overline{v}$
MONSOON-77 (PHASE-I)																
Wind at																
10m height (m/s)	5	1	12	1	4	1	10	2	4	1	9	1	6	1	13	1
Current at																
25m depth (cm/s)	−5	5	0	0	—	—	—	—	—	—	—	—	16	16	−8	8
50m Do	−9	9	−1	1	−7	32	22	28	5	33	−39	30	24	24	18	23
100m Do	−16	16	6	6	−3	3	2	2	13	18	−19	20	0	22	18	23
150m Do	—	—	—	—	−6	6	5	5	11	20	−13	18	−8	8	9	9
200m Do	−9	9	3	3	−7	8	6	7	11	19	−5	18	−8	8	6	6
MONSOON-77 (PHASE-II)																
Wind at																
10m height (m/s)	5	1	11	3	—	—	—	—	5	1	10	3	6	1	12	2
Current at																
25m depth (cm/s)	11	47	−10	44	—	—	—	—	18	40	−17	39	20	31	−13	31
50m Do.	3	36	−14	35	—	—	—	—	—	—	—	—	30	28	−15	32
100m Do	−7	25	−12	25	—	—	—	—	—	—	—	—	18	25	−1	26
150m Do	−3	11	0	11	—	—	—	—	—	—	—	—	13	21	3	22
200m Do	−2	10	0	10	—	—	—	—	—	—	—	—	6	11	2	11

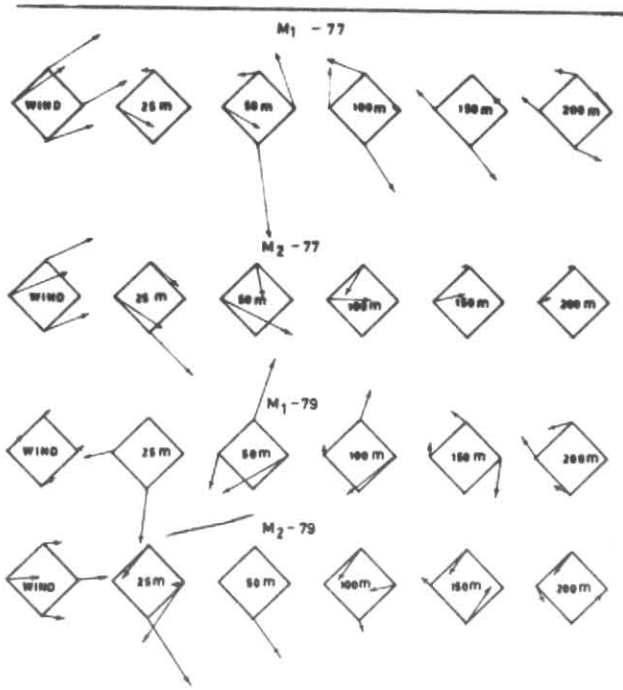

Fig. 7. Vector averaged surface wind and subsurface currents at all polygons during MONSOON-77 and MONEX-79

ocean dynamics rather than the local wind forcing alone, in the evolution of the sub-surface current field in the central Arabian Sea during the pre-onset and onset regimes of the summer monsoon.

The vector mean and standard deviation of zonal and meridional components of surface winds and subsurface currents at all depths and locations for MONSOON-77 and MONEX-79 are shown in Tables 1 (a & b). The resultant of u and v shows the mean speed and direction of the flow (Fig. 7). The currents at 25 m are considered here as the near-surface currents for a comparison with the climatological ship drift vectors. The present observations showed different current regimes at different locations during M1-77 and M2-79 (first 3 weeks of June) which are not in conformity with the climatological flow (nearly easterly) in the central Arabian Sea during June (Wyrtki 1971, Cutler and Swallow 1984, Rao *et al.* 1989). This mismatch is attributed to highly time varying near-surface

TABLE 1 (b)

	N				E				S				W			
	σu	$\bar{u}$	σv	$\bar{v}$	σu	$\bar{u}$	σv	$\bar{v}$	σu	$\bar{u}$	σv	$\bar{v}$	σu	$\bar{u}$	σv	$\bar{v}$
MONEX-79 (PHASE-I)																
Wind at																
10m height (m/s)	−1	3	−1	2	−1	3	−2	2	−3	2	−2	2	−3	3	−3	2
Current at																
25m depth (cm/s)	—	—	—	—	—	—	—	—	−1	21	−22	19	11	32	−3	34
50m Do	7	19	24	14	−27	17	−16	22	—	—	—	—	−2	20	−14	23
100m Do	4	17	12	15	−18	12	−18	16	−3	18	3	17	−1	16	4	17
150m Do	−6	17	4	16	−2	14	−16	15	—	—	—	—	0	14	6	16
200m Do	−10	15	−4	15	—	—	—	—	−6	12	4	14	−6	13	9	16
MONEX-79 (PHASE-II)																
Wind at																
10m height (m/s)	−4	5	0	−3	−6	5	0	−3	−5	4	0	−3	−7	3	0	−3
Current at																
25m depth (cm/s)	−10	13	−13	14	−16	21	−24	19	18	24	−27	28	—	—	—	—
50m Do.	—	—	—	—	−11	18	2	19	11	23	−15	28	−21	17	1	22
100m Do	−9	11	−13	14	—	—	—	—	1	20	−4	19	—	—	—	—
150m Do	−7	12	−10	11	—	—	—	—	10	15	15	16	−4	17	3	14
200m Do	−8	9	−9	10	—	—	—	—	12	14	12	12	2	10	−6	10
EQUATORIAL STATION																
Wind at																
10m height (m/s)	1	2	5	2	—	—	—	—	—	—	—	—	—	—	—	—
Current at																
25m depth (cm/s)	−10	29	−51	22	—	—	—	—	—	—	—	—	—	—	—	—
50m Do	−4	22	−68	27	—	—	—	—	—	—	—	—	—	—	—	—
100m Do	−8	23	21	19	—	—	—	—	—	—	—	—	—	—	—	—
150m Do	−31	16	−11	12	—	—	—	—	—	—	—	—	—	—	—	—
200m Do	−32	18	17	11	—	—	—	—	—	—	—	—	—	—	—	—

current field in the central Arabian Sea during the onset regime of the summer monsoon. During May 1979, the surface winds were almost southerly with a speed of ~5 m/s at EQ-79, in agreement with the climatological wind field at this location (Rao *et al.* 1991). However, the near-southerly current (speed 52 cm/s) at 25 m depth did not compare well with the climatological easterly currents at the surface (Cutler and Swallow 1984, Rao *et al.* 1991). During M2-77 (July), the observed current directions were in agreement with the climatological values implying a near-steady state conditions.

Both the σu and σv exhibited a variation within the average range of ±29 cm/s with higher values within the near-surface isothermal layer. The direction of the zonal flow ($\bar{u}$) at all depths was westerly with higher magnitudes at 150 and 200 m depths. On the other hand, the direction of the meridional currents ($\bar{v}$) changed intermittently below 50 m

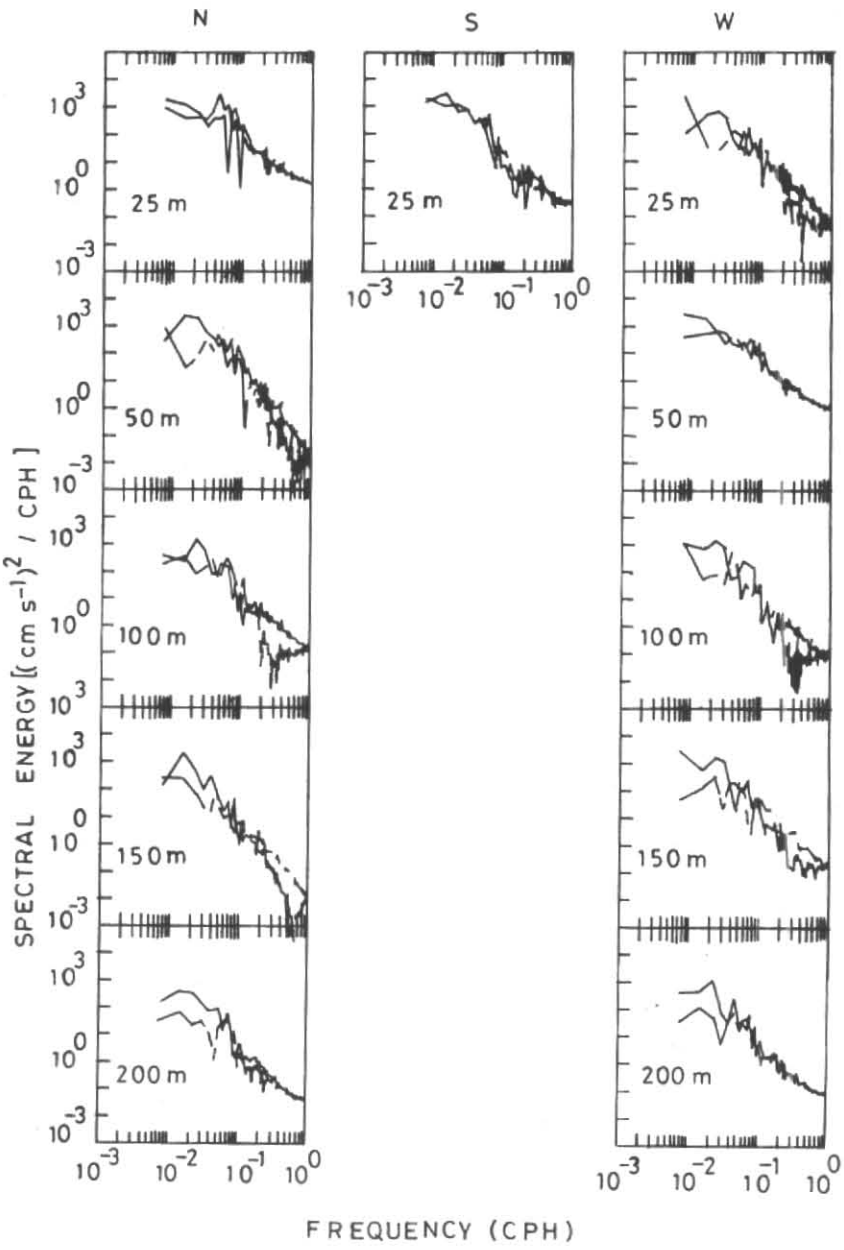

Fig. 8. Rotary spectra at all locations during M2-77. Clockwise and anticlockwise spectra are represented by continuous and broken lines respectively

depth (southerly in the upper 50 and at 150 m depth; northerly at 100 and 200 m depths). At EQ-79, the opposing currents below 100 m depth appear to have produced stronger mixing causing a weaker thermocline/pycnocline between 125 and 200 m depth (Fig. 2).

3.4. *Rotary spectra*

Rotary spectra were computed to examine the distribution of energy over a range of frequencies, positive corresponding to velocity vectors that rotate anti-clockwise with time and negative corresponding to velocity vectors that rotate clockwise with time. The clockwise (continuous line) and anticlockwise (dashed line) spectral estimates are presented in Figs. 8, 9 (a & b) and 10 for M2-77, M1-79 and M2-79 respectively. Due to short length of current meter records during M1-77, the rotary spectra could not be computed. During M2-77 the rotary spectra showed greater energy in the clockwise band compared to the anticlockwise band (Fig. 8). The

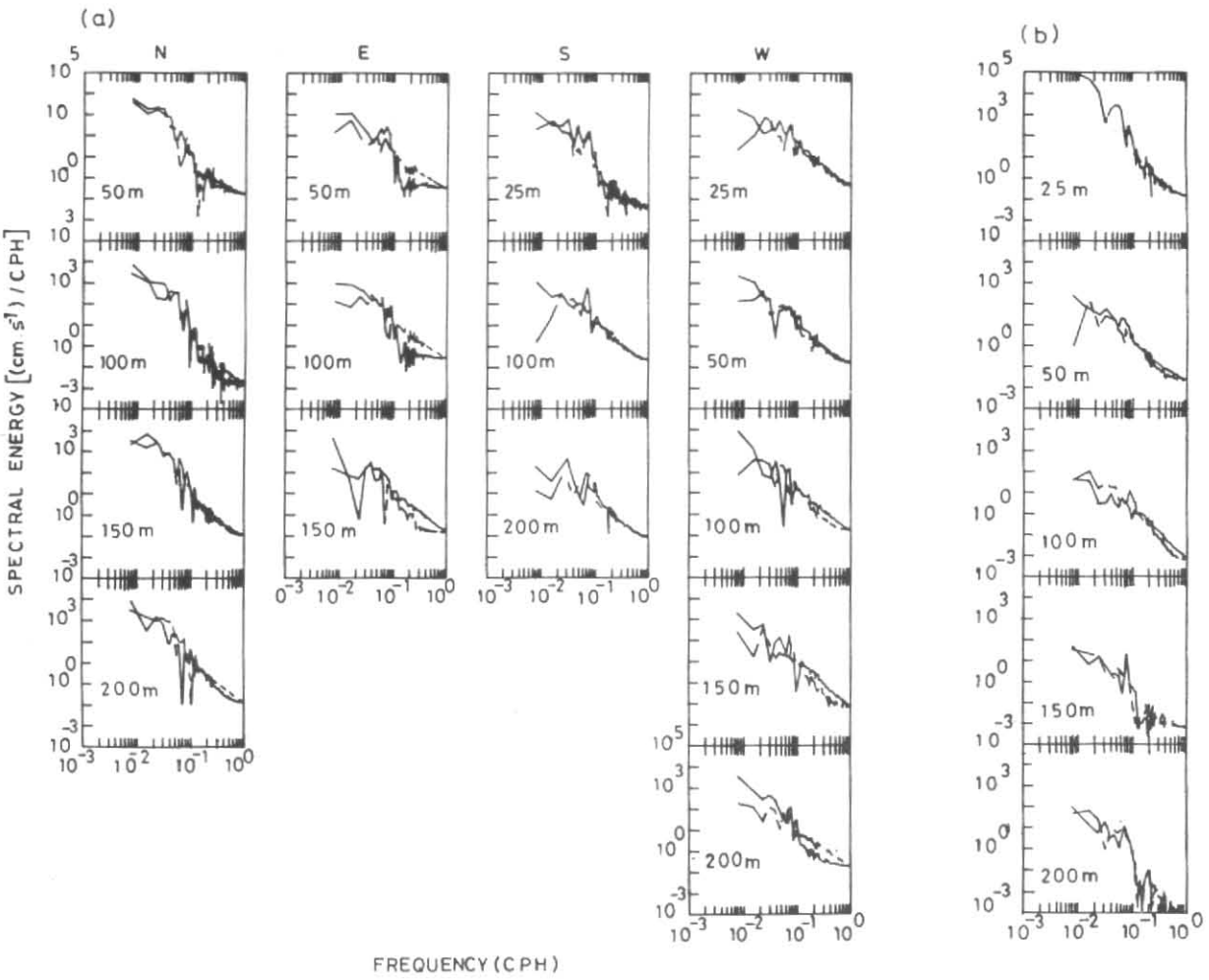

Fig. 9. Rotary spectra at all locations during M1-79. Clockwise and anticlockwise spectra are represented by continuous and broken lines respectively

estimates of the clockwise spectra showed peaks mostly corresponding to inertial, diurnal and semi-diurnal periods while the inertial peak is absent in the anticlockwise spectra as the inertial flow is clockwise in the northern hemisphere.

In general the inertial peak is dominant in the clockwise spectra at all locations during M1-79 (Fig. 9). However, the spectral energy was lower during M1-79 and M2-79 (Fig. 10) except at EQ-79 (Fig. 9) where the inertial flow is absent. Pollard and Millard (1970) successfully demonstrated the importance of local wind forcing on the amplitude of inertial oscillations beneath the mixed layer. During both MONSOON-77 and MONEX-79, the peaks corresponding to semi-diurnal periods are well resolved in both clockwise and anticlockwise spectra revealing the importance of tidal forcing. In addition to these, peaks corresponding to 16-21 hrs are also noticed both in the clockwise and anticlockwise spectra during both MONSOON-77 and MONEX-79, although their forcing mechanisms remain unknown.

4. Conclusions

In general, although the surface wind field was steady across the polygons, the subsurface current field showed a great deal of variability superposed with energetic oscillations corresponding to semi-diurnal, diurnal and inertial periods. A great deal of coherence in the vertical was noticed on these time scales although the current strength decayed with depth at certain locations due to differences in the stratification. During the onset regime, Ekman balance was not noticed between the surface wind field and near-surface flow field suggesting the importance of internal ocean dynamics both local and remote. A clear Ekman balance was noticed only during the progress regime of the monsoon when the near-surface flow field was adjusted to summer monsoonal forcing.

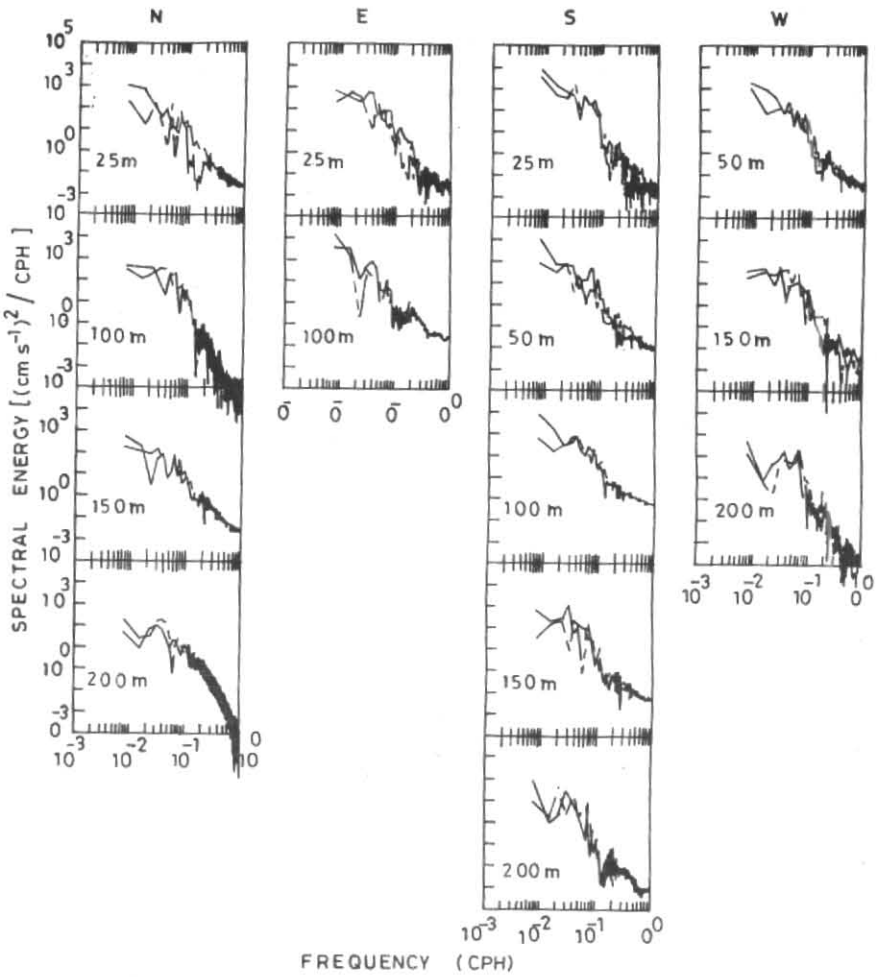

Fig. 10. Rotary spectra at all locations during M2-79. Clockwise and anticlockwise spectra are represented by continuous and broken lines respectively

Fluctuations in the flow field were dramatic at the equatorial station under the influence of developing Somali Current System with its rich eddy field. The rotary spectral analysis indicated the dominance of inertial period in the clockwise spectra, while the semi-diurnal period is prominent in both clockwise and anticlockwise spectra during both MONSOON-77 and MONEX-79.

Acknowledgements

The authors wish to record their sincere appreciation to all scientists and technicians who contributed to the collection and processing of the data sets utilised in this study. Thanks are due to Director, IMMC, New Delhi for supplying these data sets. The authors are grateful to Director, Naval Physical and Oceanograpahic Laboratory for providing the necessary facilities and constant encouragement to carryout this study. The authors appreciate the helpful comments of an anonymous referee.

References

Anderson, D. L. T. and Carrington, D. J., 1993, "Modelling inter annual variability in the Indian Ocean using momentum fluxes from the operational weather analyses of the United Kingdom Meteorological Office and European Centre for Medium Range Weather Forecasts", *J. Geophys. Res.*, **98**, 12483-12500.

India Met. Deptt., 1978, "Weather", *Indian J. Met. Hydrol. Geophys.*, **29**, 573-582.

Awade, S. T., Totagy, M. Y. and Bawiskar, S. M., 1986, "Large scale features of the summer monsoon during 1979", *Mausam*, **37**, 441-450.

Bloomfield, P., 1976, "Fourier analysis of time series: An Introduction", John Wiley & Sons, New York, p. 258.

Cox, M. D., 1970, "A mathematical model of the Indian Ocean", *Deep-Sea Res.*, **17**, 47-75.

Cutler, A. N. and Swallow, J. C., 1984, Surface currents of the Indian Ocean (to 25S, 100E) : compiled from historic data archieved by the Meteorological Office, Institute of Ocean Sciences, Wormley, U.K., Rept. 187, p. 8 and 36 charts.

Duing, W., 1970, The monsoon regime of currents in the Indian Ocean. East-West Center Press, Honolulu, p. 68.

Gonella, J., 1972, "A rotary-component method for analysing meteorological and oceanographic vector time series", *Deep-Sea Res.*, **19**, 833-846.

Gopalakrishna, V. V. and Sastry, J. S., 1986, "Surface circulation over the shelf off the east coast of India during the south west monsoon", *Indian J. Mar. Sci.*, **14**, 60-65.

Gopalakrishna, V. V., Sadhuram, Y., Ramesh Babu, V. and Rao, M. V., 1989, "Variability of windstress and currents at selected locations over the north Indian ocean during 1977 and 1979 summer monsoon seasons", *Mausam*, **39**, 159-166.

Joseph, M. G., Hareesh Kumar, P. V. and Basil Mathew, 1990, "Short term pre-onset southwest monsoonal transformations in upper western equatorial Indian Ocean", *Indian J. Mar. Sci.*, **19**, 251-256.

KNMI, 1952, Indische Ocean Oceanographische and Meteorologische gegevens. 2 Ed. Publ. No. 135, I, 31 pp. and II, 24 charts.

Knox, R. A., 1976, "On a long series of measurements of Indian Ocean equatorial currents near Addu Atoll", *Deep-Sea Res.*, **23**, 211-221.

Krishna Rao, P., 1974, "Surface circulation features in the Bay of Bengal as seen in ERTS imagery", *Mahasagar*, **7**, 1-13.

Leetma, A. and Stommel, H., 1980, "Equatorial current observations in the western Indian Ocean : 1975 and 1976", *J. Phys. Oceanogr.*, **10**, 256-269.

Leetma, A., Quadfasel, D. R. and Wilson, D., 1982, "Development of flow field during the onset of the Somali Current", *J. Phys. Oceanogr.*, **12**, 3281-3293.

Legeckis, R., 1987, "Satellite observations of a western boundary current in the Bay of Bengal", *J. Geophys. Res.*, **92**, 12974-12979.

Lighthill, M. J., 1969, "Dynamic response of the Indain Ocean to the onset of southwest monsoon", *Phil. Tran. R. Soc. London*, **A265**, 45-92.

Luther, M. E. and O'Brien, J. J., 1985, "A model of the seasonal circulation in the Arabian Sea forced by observed winds", *Prog. Ocean.*, **14**, 353-385.

Luyten, J. R. and Swallow, J. C., 1976, "Equatorial Undercurrents", *Deep-Sea Res.*, **23**, 999-1001.

McCreary, J. P., Kundu, P. K. and Molinari, R. L., 1993, "A numerical investigation of dynamic, thermodynamic and mixed-layer processes in the Indian Ocean", *Prog. Oceanogr.*, **31**, 181-244.

Molinari, R. L., Olson, D. and Reverdin, G., 1990, "Surface current distribution in the tropical Indian Ocean derived from compilations of surface buoy trajectories", *J. Geophys. Res.*, **95**, 7217-7238.

Pollard, R. T. and Millard, R. C., 1970, "Comparison between observed and simulated inertial oscillations", *Deep-Sea Res.*, **17**, 813-821.

Raniam, K. V. S., Rao, C. V. K. P. and Prasad, N. D., 1982, "On time varying currents and hydrographic conditions in the central Arabian Sea during summer monsoon — 1977", *Mausam*, **33**, 451-458.

Rao, D. P. and Sastry, J. S., 1981, "Circulation and distribution of some hydrographical properties during the late winter of the Bay of Bengal", *Mausam*, **14**, 1-16.

Rao, R. R., 1987, "The observed variability of the cooling and deepening of the mixed layer in the central Arabian Sea during MONSOON-77", *Mausam*, **38**, 43-48.

Rao, R. R., Molinari, R. L. and Festa, J. F., 1989, "Evolution of the climatological near-surface thermal structure of the tropical Indian Ocean I : Description of mean monthly mixed layer depth, sea surface temperature, surface current and surface meteorological fields", *J. Geophys. Res.*, **94**, 10801-10815.

Rao, R. R., Molinari, R. L. and Festa, J. F., 1991, "Surface meteorological and near surface oceanographic atlas of the tropical Indian Ocean", NOAA Tech. Memo. ERL AOML-69, p. 59.

Rao, R. R. and Sanilkumar, K. V., 1991, "Evolution of salinity field in the upper layers of the east central Arabian Sea and the northern Bay of Bengal during summer monsoon experiments", Proc. Indian Acad. Sci. (Earth Planet. Sci.), **100**, 69-78.

Rao, R. R., Sanilkumar, K. V. and Basil Mathew, 1991, "Observed variability in the current field during summer monsoon experiments — Part I : northern Bay of Bengal", *Mausam*, **42**, 17-24.

Schott, F., 1983, "Monsoon response of the Somali Current and associated upwelling", *Progr. Oceanogr.*, **12**, 357-381.

Schott, F., Reppin, J., Fisher, J. and Quadfasel, D., 1994, "Currents and transports of the monsoon current south of Sri Lanka", *J. Geophys. Res.*, **99**, 25127-25141.

Swallow, J. C., Molinari, R. L., Bruce, J. G., Brown, O. B. and Evans, R. H., 1983, "Development of the near-surface flow pattern and watermass distribution in the Somali Basin in response to the southwest monsoon of 1979", *J. Phys. Oceanogr.*, **13**, 1398-1415.

U.S. Navy, 1976, Marine Climatic Atlas of the World, Vol. III, Indian Ocean, 248 pp.

Varadachari, V. V. R., Murthy, C. S. and Das, P. K., 1968, "On the level of least motion and the circulation in the upper layers of Bay of Bengal", *Bull. Natl. Inst. India*, **Part I**, 301-307.

Wyrtki, K., 1971, Oceanographic atlas of the International Indian ocean expedition, Washington, D.C., p. 531.